JACS
JOURNAL OF THE AMERICAN CHEMICAL SOCIETY
Communication
pubs.acs.org/JACS

Thermodynamic-Driven Self-Assembly: Heterochiral Self-Sorting and Structural Reconfiguration in Gold(I)−Sulfido Cluster System

Liao-Yuan Yao, Terence Kwok-Ming Lee, and Vivian Wing-Wah Yam*

Institute of Molecular Functional Materials (Areas of Excellence Scheme, University Grants Committee (Hong Kong)) and Department of Chemistry, The University of Hong Kong, Pokfulam Road, Hong Kong, P. R. China

Supporting Information

ABSTRACT: By employing chiral precursors, a new class of chiral gold(I)−sulfido clusters with unique structures has been constructed. Interestingly, pure enantiomers of the precursors are found to self-assemble into chiral hexa- and decanuclear clusters sequentially, while a racemic mixture of them has resulted in heterochiral self-sorting of an achiral *meso* decanuclear cluster. Chirality has determined not only the symmetry and structures but also the photophysical behaviors of these clusters. The racemic mixture of decanuclear clusters undergoes rearrangement and heterochiral self-sorting to give a *meso* decanuclear cluster. The thermodynamic-driven heterochiral self-sorting of gold(I) clusters provides a means to develop controlled self-assembly that may be of relevance to the understanding of chirality in nature.

Among the family of gold complexes,[1] the study of gold(I) clusters, being one of the most important classes, has attracted considerable attention in recent decades.[2] In the polynuclear gold(I) assemblies, aurophilic interactions[3] have not only supported their diverse cluster architectures, but also have endowed them with attractive structure-dependent photophysical behavior,[4−6] which are also frequently observed in metal nanoparticles and quantum dots.[7] Recently, besides the structures, there has also been an emerging interest in the applications of gold(I) clusters, such as luminescence,[2e,4d,5c,f] catalysis,[1c,2a,8a] chemosensing,[5e,6a,f] structural rearrangement,[5f,6b,d] nanoaggregates,[6c] medicine,[1b,5b] biomimetics,[1a,b,8b] and so on. The stability and ready availability of polynuclear sulfido gold(I) complexes[2b,4b−d,6a−d] have enabled them to be one of the most attractive candidates for various application studies.

Supramolecular self-assembly and chiral self-sorting behaviors are ubiquitous in nature.[9] For instance, the quaternary structure of proteins is constructed in a stepwise manner by noncovalent interactions, while the chiral double helical structure of DNA is self-sorted through hydrogen bonding. Artificial systems with an understanding of the control of size and shape as well the handedness can help to provide insights into the mechanism of the precise control and organization as well as the recognition behavior and the origin of chirality in nature.[10] Sequential self-assembly has been widely observed in polymers and in nanoscience.[11] It is still a major challenge to have a precise control over homochiral and heterochiral self-sorting of the systems.[9b,c,12a] Although there have been a limited number of examples on heterochiral self-sorting reported in the organic systems,[10e,12a,b] heterochiral self-sorting involving metal−organic assemblies has been much less explored and rarely reported.[12c] Furthermore, to our knowledge, it is not common to have both sequential self-assembly and heterochiral self-sorting in the same artificial system, not even to mention the gold(I) cluster system.

The importance of hydrogen bonding in nature and the comparable energy of aurophilic interactions to hydrogen bonding have enabled the gold(I) assemblies to serve as a promising alternative in artificial systems, especially for those that are of relevance to biological processes, such as self-assembly and self-discrimination. Herein, we successfully develop an unprecedented chiral polynuclear μ_3-sulfido gold(I) cluster system. By employing chiral chlorogold(I) precursors, the chiral hexa- and decanuclear clusters that share the same [Au_3S] basic building blocks have been assembled sequentially. Surprisingly, by replacing the enantiomers of chiral precursors with a racemic mixture, a different *meso* achiral decanuclear gold(I) μ_3-sulfido cluster, rather than a racemic mixture of chiral decanuclear clusters, was obtained instead through heterochiral self-sorting. The chirality of these clusters has not only determined their symmetry and structures but also reveals their attractive structure-dependent photophysical properties. Most interestingly, the racemic mixture of chiral decanuclear clusters has been found to undergo rearrangement and self-sorting to give the achiral *meso*-cluster in solution, indicating the thermodynamic nature of the heterochiral self-sorting, which provides a basis for the future exploration of various potential applications and for the future design of new biomimetic artificial systems.

Reaction of *R*- or *S*-[BINAP$(AuCl)_2$] (**1*R*** or **1*S***) (Figure 1a) with H_2S in dichloromethane/ethanol/pyridine using a procedure previously reported by us for nonchiral luminescent gold(I) clusters[4b−d,6a−d] gave rise to chiral decanuclear gold(I) clusters (**2*R*** or **2*S***). The dicationic molecular peak (m/z = 2293.6) in electrospray ionization mass spectrometry (ESI-MS) establishes their chemical formula as [Au_{10}(*R*-BINAP)$_4$(μ_3-S)$_4$]Cl_2 (**2*R***) or [Au_{10}(*S*-BINAP)$_4$(μ_3-S)$_4$]Cl_2 (**2*S***) (Figure S1). Unlike previous decanuclear gold(I) clusters,[4c,6b−d] the $^{31}P\{^1H\}$ NMR spectra of **2*R*** and **2*S*** both show two singlets at δ 24.3 and 38.4 ppm (see Figure S1 inset), rather than a pair of doublets as reported previously, indicating the adoption of a different structure. Single crystal X-ray analyses of **2*R*** and **2*S*** reveal their unique four-leaf clover-shaped decanuclear structures (Figure 1b). In these chiral decanuclear clusters, the six Au(I) atoms in

Received: April 14, 2016
Published: June 1, 2016

DOI: 10.1021/jacs.6b03844
J. Am. Chem. Soc. 2016, 138, 7260−7263

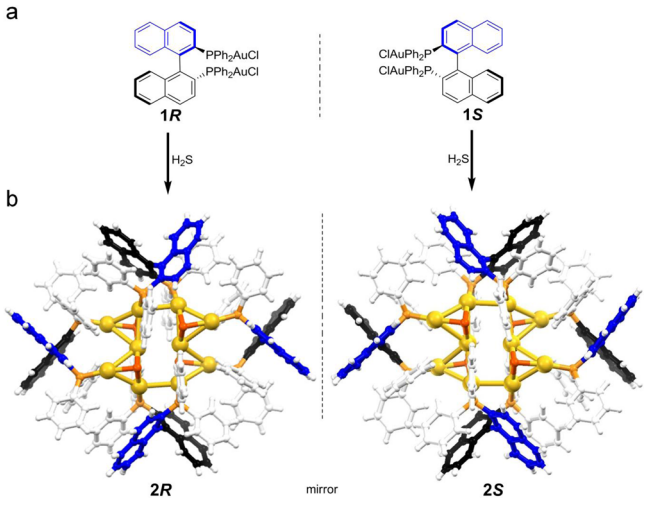

Figure 1. (a) Chiral BINAP-based dinuclear precursors, **1*R*** and **1*S***. (b) X-ray structures of chiral decanuclear gold(I)−sulfido clusters, **2*R*** and **2*S*** (Au, yellow; S, red; P, orange; H and C, white; for clarity, the BINAP rings are shown in black (below plane of paper) and blue (above paper) and the counter-anions and solvent molecules are omitted.).

the middle are located on nearly one plane to form a rectangle. Compared to the contacts (ca. 3.0 Å) at the short edges of the rectangle, relatively long Au···Au distances (ca. 3.3 Å) are found between the two central gold(I) atoms (Tables S1 and S2). The other four Au(I) atoms are attached above or below the rectangular plane by Au−S bonds and Au···Au interactions (Tables S1 and S2). The decanuclear cluster can also be viewed as containing two sets of double triangles, each of which has two $[Au_3S]$ pyramids sharing one common gold(I) atom. Both the chiral cluster molecules and their decanuclear gold(I) cores possess a local chiral D_2 symmetry. Chiral gold(I) clusters with chiral metal cores in the same symmetry group are not very common. The chirality has been transferred from and amplified by the axial chiral BINAP ligands to the gold(I) cluster cores.

Surprisingly, reaction of *rac*-$[BINAP(AuCl)_2]$ (**1-*rac***) and H_2S under the same conditions is found to give a new cluster complex as a yellow solid of more distinct color and different NMR response (Figure S2). The molecular formula and the structure of this complex have been finalized by X-ray single crystal structure analysis as $[Au_{10}(R\text{-BINAP})_2(S\text{-BINAP})_2(\mu_3\text{-S})_4]Cl_2$ (**2-*meso***), a novel *meso* decanuclear gold(I)−sulfido cluster supported by alternating *R*- and *S*-BINAP ligands (Figure S3). Different from the chiral decanuclear gold(I) clusters (**2*R*** and **2*S***), complex **2-*meso*** consists of a propeller-shape assembly with ideal S_4 point group symmetry both in the solution and crystal states. Similar to the previously reported decanuclear clusters with nonchiral diphosphine ligands,[4c,6b−d] **2-*meso*** also possesses a Au_{10} core with a Au_8 macrocycle containing a Au_2 chain at the center. They adopt the same propeller-shape structure with S_4 symmetry, indicating the optimality of this structure pattern.

Occasionally, during the recrystallization of **2*S*** for single crystal analysis, colorless prism crystals are found; one of the crystals was picked for X-ray single crystal determination, which reveals its identity as a unique hexanuclear gold(I) cluster, $[Au_6(S\text{-BINAP})_3(\mu_3\text{-S})Cl_3]Cl$ (**3*S***) (Figure S3). This hexanuclear cluster contains three *S*-BINAP ligands, six Au(I) atoms, and one sulfide atom, resembling the shape of a "clover". The $^{31}P\{^1H\}$ NMR spectra of the hexanuclear clusters show a pair of doublets with P−P coupling (Figures S2 and S4), indicating the different phosphorus environments in the same BINAP ligand. Based on these results, a local chiral C_3 symmetry has been assigned to **3*R*** and **3*S***.

Decanuclear clusters **2-*meso*** and **2*R*/*S***, having the same chemical formula but different structures and symmetry (Figure S5), have provided an excellent opportunity for the exploration of interesting structure-dependent photophysical properties. The chiral decanuclear gold(I) clusters, **2*R*** and **2*S***, only absorb UV light with wavelengths of less than 400 nm, with an absorption shoulder at about 339 nm and their solutions are colorless (Figure 2a and Figure S6). In contrast, a lower energy ^{1}LMMCT

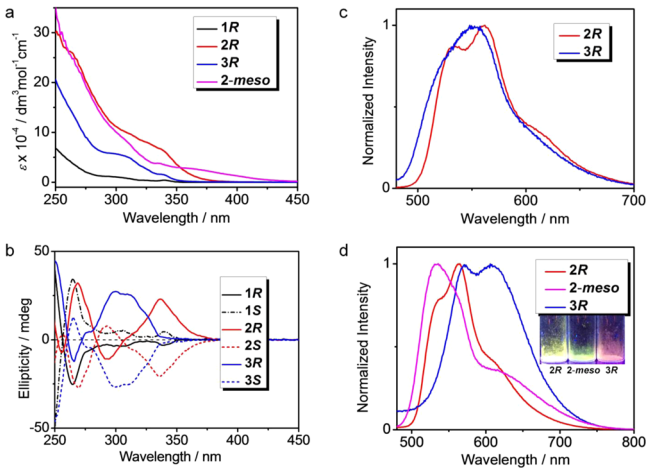

Figure 2. (a) UV−vis spectra of **1*R***, **2*R***, **2-*meso***, and **3*R***. (b) CD spectra of chiral gold(I) complexes, **1*R***, **1*S***, **2*R***, **2*S***, **3*R***, and **3*S***. (c) Emission spectra of **2*R*** and **3*R*** in solution. (d) Solid state emission spectra of **2*R***, **2-*meso***, and **3*R*** at room temperature (the inset shows the photographs of their emission color).

absorption shoulder at 364 nm, with a tail in the visible region at about 400−450 nm is observed in the UV−vis absorption spectrum of the achiral decanuclear cluster **2-*meso***, giving a yellow solution (Figure S6). The CD-silence of **2-*meso*** has confirmed its achiral nature. Conversely, the CD spectra of **2*R*** and **2*S*** display intense Cotton effects and a mirror image relationship in the range of 250−380 nm, which establishes their chiral configurations (Figure 2b). Besides the chiral BINAP ligands, the chiral metal cores are believed to also contribute to the origin of the CD signals of the chiral clusters.

Chiral decanuclear gold(I) clusters **2*R*** and **2*S*** show structured and long-lived ^{3}IL luminescence in dichloromethane, with photoluminescence quantum yield of around 2% (Figure 2c and Table S6). In contrast, *meso* decanuclear cluster **2-*meso*** is nonemissive in solution (Figure S6) but gives a dual green and orange emission in the solid state both at ambient temperature and at low temperature (77 K) upon excitation (Figure 2d and Table S6). The low-energy emission band for **2-*meso*** and **3*R*/*S*** at around 610−620 nm has been assigned as triplet ligand-to-metal charge transfer excited state (^{3}LMCT) modified by metal···metal interactions,[4c,6b] whereas the structured emission commonly observed in the BINAP systems[13] is assigned as triplet metal-perturbed intraligand (^{3}IL) phosphorescence. Altering combinations of the chiral ligands affects their structural pattern, symmetry, and Au(I)···Au(I) interactions, leading to unusual and unique structure-dependent photophysical properties and emission origins (Figure 2).

The structure analysis shows that in hexanuclear clusters **3*R*** and **3*S*** not all Cl−Au(I) coordination has been replaced by S−

DOI: 10.1021/jacs.6b03844
J. Am. Chem. Soc. 2016, 138, 7260−7263

Au(I) coordination. This indicates that the hexanuclear gold(I) clusters are available to undergo additional reaction and assembly. For better control of the stoichiometric addition, lithium sulfide was used instead of hydrogen sulfide as the sulfide source. Upon addition of lithium sulfide, a pair of doublets and a pair of singlets are observed at δ 26.0 and 35.7 ppm and δ 25.8 and 35.6 ppm sequentially in $^{31}P\{^{1}H\}$ NMR spectra (Figure 3a),

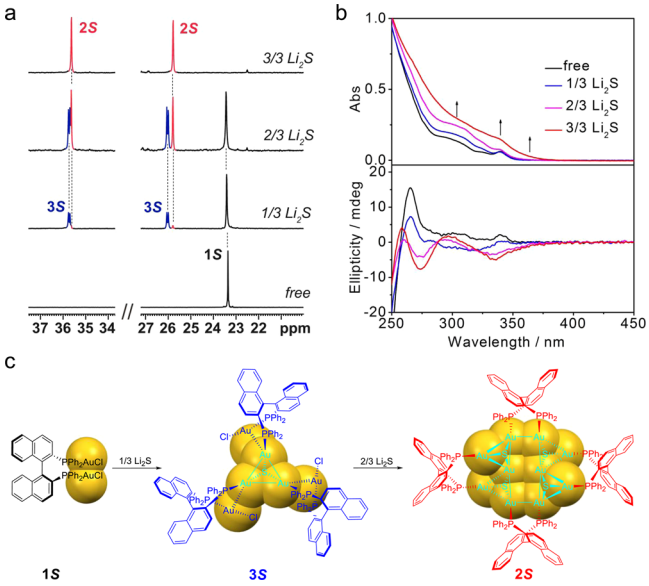

Figure 3. (a) $^{31}P\{^{1}H\}$ NMR monitoring of the assembly process (1 mM in $CDCl_3$). (b) UV–vis (upper) and CD (lower) spectral changes upon the addition of Li_2S to **1*S*** (11 μM in $CHCl_3$). (c) Scheme showing the self-assembly process from dinuclear precursor **1*S*** to hexanuclear cluster **3*S*** and to decanuclear cluster **2*S***. All the equivalents of Li_2S here, such as 1/3, 2/3, and 3/3, are based on the precursor **1*S***.

indicating the formation of hexanuclear cluster **3*S*** and decanuclear cluster **2*S***. When the amount of sulfide reaches an equivalent of **1*S***, signals characteristic of **1*S*** and **3*S*** disappear completely, and only signals due to **2*S*** remain. UV–vis along with CD spectral changes are also observed during the assembly process, corresponding to the sequential formation of hexa- and decanuclear clusters (Figure 3b). Similar sequential assembly process has been observed for their *R* enantiomers (Figure S7). The hexagold(I) clusters **3*R*** and **3*S*** are key intermediates in the assembly of chiral clusters **2*R*** and **2*S***. The main framework of **3*R*/*S*** is the [Au_3S] pyramid, which is also the fundamental building block of **2*R*/*S*** (Figure 3c).

Attempts have been made to obtain a racemic mixture of chiral decanuclear gold(I) clusters through homochiral self-sorting from **1-*rac***. However, a clear yellow solution instead of a pale yellow solution of **2*R*/*S*** is obtained. NMR and ESI–MS studies indicate that the product is a decanuclear gold(I) cluster with structure different from that of **2*R*/*S***. Theoretically, if the self-assembly process is completely random, the combination of BINAP ligands can be (*RRRS*), (*RSRS*), (*RRSS*), and (*RSSS*) (Figure 4a), which is difficult to differentiate. Fortunately, single crystals are obtained and X-ray analysis finally establishes a *meso* decanuclear gold(I) cluster **2-*meso*** with the alternating *R*- and *S*-BINAP ligands (*RSRS*), revealing the existence of an interesting heterochiral self-sorting phenomenon (Figure 4b). Most interestingly, a racemic mixture of **2*R*** and **2*S*** can undergo further self-sorting into achiral cluster **2-*meso*** through structural reconfiguration of the clusters in solution (Figure 4b). The

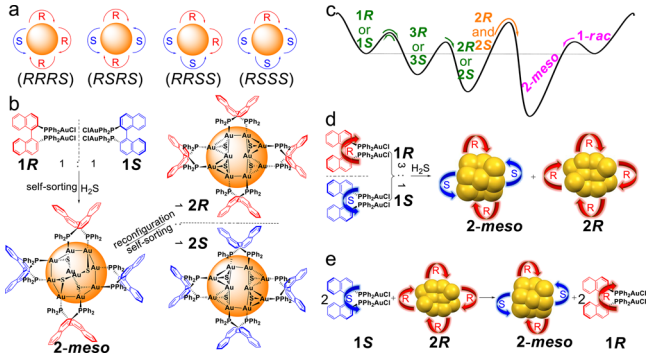

Figure 4. (a) Illustration of possible combinations of the chiral ligands during random assembly. (b) Scheme showing self-sorting from the racemic precursor and chiral cluster. (c) Proposed energy profile during the assembly process. (d) Self-discrimination between precursors **1*R*** and **1-*rac*** during the assembly, starting from **1*R*/1*S*** = 3:1 (also **1*R*/1-*rac*** = 1:1) mixture. (e) Displacement reaction via heterochiral self-sorting.

structural reconfiguration and heterochiral self-sorting from a mixture of **2*R*** and **2*S*** to *meso* decanuclear cluster **2-*meso*** have been monitored by UV–vis spectroscopy in solution, and the growth of absorbance at around 400 nm is characteristic of the existence of heterochiral self-sorting (Figure S8).

From these studies, **2-*meso*** is found to be thermodynamically more stable than the racemic mixture of enantiomers **2*R*** and **2*S***. This provides the driving force for the highly selective heterochiral self-sorting-induced structural reconfiguration. The slow reaction rate may be attributed to the higher energy barrier between the racemic and the *meso* gold(I) clusters caused by aurophilic interactions. Since **3*R*** and **3*S*** tend to undergo disproportionation reaction to their precursors as revealed by NMR studies, the chiral hexanuclear gold(I) clusters are supposed to be the kinetic metastable intermediates, and their energy levels are proposed to be between those of **1*R*/*S*** and **2*R*/*S*** (Figure 4c). Not only the photophysical behaviors but also the stability and reactivity have been influenced by the structures and symmetry of these gold(I) clusters, which are dramatically distinct between the homochiral and heterochiral clusters.

To further reveal the thermodynamic nature of the heterochiral self-sorting, the following experiments have been designed and carried out. A mixture of **1*R*** and **1*S*** in a mole ratio of 3:1 (also **1*R*/1-*rac*** = 1:1) under a H_2S atmosphere results in nearly equal equivalents of **2*R*** and **2-*meso*** (Figure 4d), which can be revealed by $^{31}P\{^{1}H\}$ NMR analysis. Additionally, stirring two equivalents of **1*S*** with **2*R*** in solution for several days leads to the appearance of two negative peaks at around 310 and 340 nm in the CD spectra, indicative of the disappearances of **2*R*** and the presence of **1*R*** (Figure S9). Meanwhile, the corresponding UV–vis spectra show a growth in absorbance in the range of 350–425 nm, indicating the formation of complex **2-*meso*** (Figure S10). This suggests that *R*-BINAP has replaced half of the original *S*-BINAP ligands on **2*R***, leading to the formation of *meso* cluster **2-*meso*** and release of chiral precursor **1*R*** in the solution (Figure 4e). These results are in line with the energy profile and further demonstrate the thermodynamic nature of this heterochiral self-sorting.

In summary, novel chiral gold(I) clusters and an achiral *meso*-cluster are reported in this work. Employing different combinations of chiral ligands alters the chirality of the resulted gold(I) complexes, leading to unusual and unique structure-dependent photophysical properties. Attractive heterochiral self-sorting and sequential self-assembly are observed and monitored

DOI: 10.1021/jacs.6b03844
J. Am. Chem. Soc. 2016, 138, 7260–7263

in this BINAP-based gold(I) cluster system. The assembly processes and structural reconfiguration are dominated by the thermodynamic-driven heterochiral self-sorting. The comparable energy of aurophilic interactions to hydrogen bonding has enabled the chiral gold(I) clusters to undergo self-assembly in a stepwise fashion and to display heterochiral self-sorting behavior. Our research would provide a fascinating model for the future design of novel chiral gold(I) clusters and artificial systems and also would be beneficial to a better understanding of the heterochiral self-sorting and assembly processes that occur in nature.

■ ASSOCIATED CONTENT

Supporting Information

The Supporting Information is available free of charge on the ACS Publications website at DOI: 10.1021/jacs.6b03844.

Synthesis and characterization, X-ray crystallography, photophysical studies, and supplementary figures (Figures S1−S15) (PDF)
Compound **2*R*** (CIF)
Compound **2*S*** (CIF)
Compound **2-*meso*** (CIF)
Compound **3*R***(CIF)
Compound **3*S*** (CIF)

■ AUTHOR INFORMATION

Corresponding Author

*wwyam@hku.hk

Notes

The authors declare no competing financial interest.

■ ACKNOWLEDGMENTS

V.W.-W.Y. acknowledges support from The University of Hong Kong under the Strategic Research Theme on New Materials. This work was supported by the ANR/RGC Joint Research Scheme (A-HKU704/12), the University Grants Committee Areas of Excellence Scheme (AoE/P-03/08), and a General Research Fund (GRF) Grant from the Research Grants Council of the Hong Kong Special Administrative Region, P. R. China (HKU 17304715). L.-Y.Y. acknowledges the receipt of a postgraduate studentship from The University of Hong Kong. Dr. Lap Szeto is acknowledged for her assistance in X-ray crystal data collection. The authors would like to thank Mr. Hao Li and Prof. Shu-Yan Yu for their assistance in mass spectrometry measurements.

■ REFERENCES

(1) (a) Schmidbaur, H. *Gold: Progress in Chemistry, Biochemistry and Technology*; John Wiley & Sons Ltd: Chichester, England, 1999. (b) Fabian, M. *Gold Chemistry: Applications and Future Directions in the Life Sciences*; WILEY-VCH Verla GmbH & Co. KGaA: Weinheim, Germany, 2009. (c) Laguna, A., Ed. *Modern Supramolecular Gold Chemistry: Gold-Metal Interactions and Applications*; Wiley: Weinheim, Germany, 2008.

(2) (a) Schmidbaur, H.; Raubenheimer, H. G.; Dobrzanska, L. *Chem. Soc. Rev.* **2014**, *43*, 345−380. (b) Gimeno, M. C.; Laguna, A. *Chem. Soc. Rev.* **2008**, *37*, 1952−1966. (c) Puddephatt, R. J. *Chem. Soc. Rev.* **2008**, *37*, 2012−2027. (d) Che, C. M.; Lai, S. W. *Coord. Chem. Rev.* **2005**, *249*, 1296−1309. (e) Yam, V. W. W.; Au, V. K. M.; Leung, S. Y. L. *Chem. Rev.* **2015**, *115*, 7589−7728.

(3) (a) Scherbaum, F.; Grohmann, A.; Huber, B.; Kruger, C.; Schmidbaur, H. *Angew. Chem., Int. Ed. Engl.* **1988**, *27*, 1544−1546. (b) Schmidbaur, H.; Schier, A. *Chem. Soc. Rev.* **2012**, *41*, 370−412. (c) Pyykkö, P. *Chem. Rev.* **1997**, *97*, 597−636.

(4) (a) Zeller, E.; Beruda, H.; Kolb, A.; Bissinger, P.; Riede, J.; Schmidbaur, H. *Nature* **1991**, *352*, 141−143. (b) Yam, V. W. W.; Cheng, E. C. C.; Cheung, K. K. *Angew. Chem., Int. Ed.* **1999**, *38*, 197−199. (c) Yam, V. W. W.; Cheng, E. C. C.; Zhou, Z. Y. *Angew. Chem., Int. Ed.* **2000**, *39*, 1683−1685. (d) Yam, V. W. W.; Cheng, E. C. C.; Zhu, N. Y. *Angew. Chem., Int. Ed.* **2001**, *40*, 1763−1765. (e) Fenske, D.; Langetepe, T.; Kappes, M. M.; Hampe, O.; Weis, P. *Angew. Chem., Int. Ed.* **2000**, *39*, 1857−1860. (f) Tzeng, B. C.; Che, C. M.; Peng, S. M. *Chem. Commun.* **1997**, 1771−1772.

(5) (a) Sevillano, P.; Fuhr, O.; Kattannek, M.; Nava, P.; Hampe, O.; Lebedkin, S.; Ahlrichs, R.; Fenske, D.; Kappes, M. M. *Angew. Chem., Int. Ed.* **2006**, *45*, 3702−3708. (b) Chui, S. S. Y.; Chen, R.; Che, C. M. *Angew. Chem., Int. Ed.* **2006**, *45*, 1621−1624. (c) Koshevoy, I. O.; Lin, C. L.; Karttunen, A. J.; Haukka, M.; Shih, C. W.; Chou, P. T.; Tunik, S. P.; Pakkanen, T. A. *Chem. Commun.* **2011**, *47*, 5533−5535. (d) Koshevoy, I. O.; Chang, Y. C.; Karttunen, A. J.; Selivanov, S. I.; Janis, J.; Haukka, M.; Pakkanen, T.; Tunik, S. P.; Chou, P. T. *Inorg. Chem.* **2012**, *51*, 7392−7403. (e) Koshevoy, I. O.; Chang, Y. C.; Karttunen, A. J.; Haukka, M.; Pakkanen, T.; Chou, P. T. *J. Am. Chem. Soc.* **2012**, *134*, 6564−6567. (f) Lasanta, T.; Olmos, M. E.; Laguna, A.; Lopez-de-Luzuriaga, J. M.; Naumov, P. *J. Am. Chem. Soc.* **2011**, *133*, 16358−16361.

(6) (a) Lee, T. K. M.; Zhu, N. Y.; Yam, V. W. W. *J. Am. Chem. Soc.* **2010**, *132*, 17646−17648. (b) Yao, L. Y.; Hau, F. K. W.; Yam, V. W. W. *J. Am. Chem. Soc.* **2014**, *136*, 10801−10806. (c) Hau, F. K. W.; Lee, T. K. M.; Cheng, E. C. C.; Au, V. K. M.; Yam, V. W. W. *Proc. Natl. Acad. Sci. U. S. A.* **2014**, *111*, 15900−15905. (d) Yao, L. Y.; Yam, V. W. W. *J. Am. Chem. Soc.* **2015**, *137*, 3506−3509. (e) Yu, S. Y.; Sun, Q. F.; Lee, T. K. M.; Cheng, E. C. C.; Li, Y. Z.; Yam, V. W. W. *Angew. Chem., Int. Ed.* **2008**, *47*, 4551−4554. (f) Jiang, X. F.; Hau, F. K. W.; Sun, Q. F.; Yu, S. Y.; Yam, V. W. W. *J. Am. Chem. Soc.* **2014**, *136*, 10921−10929.

(7) (a) Fernando, A.; Dimuthu, K. L.; Weerawardene, M.; Karimova, N. V.; Aikens, C. M. *Chem. Rev.* **2015**, *115*, 6112−6216. (b) Nozik, A. J.; Beard, M. C.; Luther, J. M.; Law, M.; Ellingson, R. J.; Johnson, J. C. *Chem. Rev.* **2010**, *110*, 6873−6890.

(8) (a) Pei, X. L.; Yang, Y.; Lei, Z.; Chang, S. S.; Guan, Z. J.; Wan, X. K.; Wen, T. B.; Wang, Q. M. *J. Am. Chem. Soc.* **2015**, *137*, 5520−5525. (b) Mohr, F.; Jennings, M. C.; Puddephatt, R. J. *Angew. Chem., Int. Ed.* **2004**, *43*, 969−971.

(9) (a) Keizer, H. M.; Sijbesma, R. P. *Chem. Soc. Rev.* **2005**, *34*, 226−234. (b) Crego-Calama, M.; Reinhoudt, D. N. *Supramolecular Chirality*; Springer-Verlag: Berlin Heidelberg, Germany, 2006. (c) Safont-Sempere, M. M.; Fernandez, G.; Wurthner, F. *Chem. Rev.* **2011**, *111*, 5784−5814.

(10) (a) He, Y.; Ye, T.; Su, M.; Zhang, C.; Ribbe, A. E.; Jiang, W.; Mao, C. D. *Nature* **2008**, *452*, 198−201. (b) O'Leary, L. E. R.; Fallas, J. A.; Bakota, E. L.; Kang, M. K.; Hartgerink, J. D. *Nat. Chem.* **2011**, *3*, 821−828. (c) Groschel, A. H.; Schacher, F. H.; Schmalz, H.; Borisov, O. V.; Zhulina, E. B.; Walther, A.; Muller, A. H. E. *Nat. Commun.* **2012**, *3*, 710. (d) Dressel, C.; Reppe, T.; Prehm, M.; Brautzsch, M.; Tschierske, C. *Nat. Chem.* **2014**, *6*, 971−977. (e) Jedrzejewska, H.; Wierzbicki, M.; Cmoch, P.; Rissanen, K.; Szumna, A. *Angew. Chem., Int. Ed.* **2014**, *53*, 13760−13764. (f) Ziegler, M.; Davis, A. V.; Johnson, D. W.; Raymond, K. N. *Angew. Chem., Int. Ed.* **2003**, *42*, 665−668. (g) Scarso, A.; Rebek, J., Jr. *Top. Curr. Chem.* **2006**, *265*, 1−46.

(11) (a) Yan, X. Z.; Li, S. J.; Cook, T. R.; Ji, X. F.; Yao, Y.; Pollock, J. B.; Shi, Y. H.; Yu, G. C.; Li, J. Y.; Huang, F. H.; Stang, P. J. *J. Am. Chem. Soc.* **2013**, *135*, 14036−14039. (b) Hudson, Z. M.; Boott, C. E.; Robinson, M. E.; Rupar, P. A.; Winnik, M. A.; Manners, I. *Nat. Chem.* **2014**, *6*, 893−898. (c) Qiu, H. B.; Hudson, Z. M.; Winnik, M. A.; Manners, I. *Science* **2015**, *347*, 1329−1332.

(12) (a) Makiguchi, W.; Tanabe, J.; Yamada, H.; Iida, H.; Taura, D.; Ousaka, N.; Yashima, E. *Nat. Commun.* **2015**, *6*, 7236. (b) Wu, A. X.; Chakraborty, A.; Fettinger, J. C.; Flowers, R. A., II; Isaacs, L. *Angew. Chem., Int. Ed.* **2002**, *41*, 4028−4031. (c) Claessens, C. G.; Torres, T. *J. Am. Chem. Soc.* **2002**, *124*, 14522−14523.

(13) Kunkely, H.; Vogler, A. *Inorg. Chem. Commun.* **1999**, *2*, 533−535.

DOI: 10.1021/jacs.6b03844
J. Am. Chem. Soc. 2016, 138, 7260−7263